Neoplasia • Vol. 9, No. 1, January 2007, pp. 8–17 8

www.neoplasia.com

Tumor-Suppressor Function of SPARC-Like Protein 1/Hevin in Pancreatic Cancer

Irene Esposito[*,1], *Hany Kayed*[†,1], *Shereen Keleg*[†], *Thomas Giese*[‡], *E. Helene Sage*[§], *Peter Schirmacher*[*], *Helmut Friess*[†] *and Jörg Kleeff*[†]

*Institute of Pathology, University of Heidelberg, Heidelberg, Germany; [†]Department of General Surgery, University of Heidelberg, Heidelberg, Germany; [‡]Institute of Immunology, University of Heidelberg, Heidelberg, Germany; [§]Hope Heart Program, Benaroya Research Institute at Virginia Mason, Seattle, WA, USA

Abstract

SPARC-like protein 1 (SPARCL1), a member of the SPARC family, is downregulated in various tumors. In the present study, the expression and localization of SPARCL1 were analyzed in a wide range of nontumorous and neoplastic pancreatic tissues by quantitative reverse transcription–polymerase chain reaction, laser capture microdissection, microarray analysis, and immunohistochemistry. For functional analysis, proliferation and invasion assays were used in cultured pancreatic cancer cells. Pancreatic ductal adenocarcinoma (PDAC) and other pancreatic neoplasms exhibited increased SPARCL1 mRNA levels compared to those of the normal pancreas. SPARCL1 mRNA levels were low to absent in microdissected and cultured pancreatic cancer cells, and promoter demethylation increased SPARCL1 levels only slightly in three of eight cell lines. SPARCL1 was observed in small capillaries in areas of inflammation/tumor growth and in some islet cells. In PDAC, 15.4% of vessels were SPARCL1-positive. In contrast, the percentage of SPARCL1-positive vessels was higher in chronic pancreatitis and benign and borderline pancreatic tumors. Recombinant SPARCL1 inhibited pancreatic cancer cell invasion and exerted moderate growth-inhibitory effects. In conclusion, SPARCL1 expression in pancreatic tissues is highly correlated with level of vascularity. Its anti-invasive effects and reduced expression in metastasis indicate tumor-suppressor function.

Neoplasia (2007) **9,** 8–17

Keywords: SPARCL1, hevin, cystic tumors, PanIN, matricellular.

Introduction

The SPARC family of proteins comprises 10 members, two of which—Secreted Protein Acidic and Rich in Cysteine (SPARC; also known as osteonectin and BM40) and SPARC-like protein 1 (SPARCL1; also known as SC1, high endothelial venule protein, or hevin)—have been implicated in the progression of a variety of tumors [1–5]. Members of the SPARC family of proteins modulate cellular functions through interactions with extracellular matrix (ECM) proteins and growth factors [6]. SPARC is implicated in the modulation of cell shape, inhibition of cell cycle, and synthesis/assembly of ECM, for example, by regulating decorin expression and collagen fibril assembly [7–10]. SPARC-deficient mice suffer from aberrations in the structure and composition of the ECM that lead to cataracts, severe osteopenia, accelerated closure of dermal wounds [11], and accumulation of adipose tissues [7].

SPARC is overexpressed in many tumors of the digestive tract, such as the colon [12], esophagus [13], and liver [14]; as well as in tumors of the breast [15], prostate [16], and bladder [17]; and in melanomas [18], astrocytomas [19], and meningiomas [20]. Together with the promotion of invasion and tumor formation, altered SPARC expression correlates with disease progression and/or poor prognosis. In pancreatic ductal adenocarcinoma (PDAC), SPARC is markedly upregulated and produced by both cancer cells and surrounding fibroblasts. Interestingly, recombinant (r) SPARC reduces pancreatic cancer cell proliferation and promotes its invasiveness *in vitro* [21].

SPARCL1 was first isolated from high endothelial cells of tonsillar venules; it is expressed in a wide range of tissues, such as tissues of the lymph node, brain, heart, lung, skeletal muscle, ovary, small intestine, and colon. SPARCL1 levels are low in the placenta, pancreas, testis, spleen, and thymus, whereas kidney, liver, and peripheral blood leukocytes are devoid of SPARCL1 [2].

SPARCL1 is downregulated in transformed prostate epithelial cell lines and metastatic prostate adenocarcinoma [22], non–small cell lung cancer [23], brain and parathyroid tumors, and is below detection levels in primary bladder, prostate, and ovarian tumors [24]. However, SPARCL1 has been identified as a marker of tumor-associated endothelium [25], but its function in human tumors is not completely understood. SPARCL1 has antiadhesive properties [2,4], and loss of SPARCL1 expression, possibly due to deletions/mutations or promoter hypermethylation [26], is associated with increased proliferative activity and cell cycle progression [24].

Address all correspondence to: Jörg Kleeff, MD, Department of General Surgery, University of Heidelberg, Im Neuenheimer Feld 110, Heidelberg 69120, Germany.
E-mail: joerg_kleeff@med.uni-heidelberg.de

[1]Irene Esposito and Hany Kayed contributed equally to this study.

Received 7 October 2006; Revised 11 November 2006; Accepted 13 November 2006.

DOI 10.1593/neo.06646

In the present study, the expression and localization of SPARCL1 were analyzed in a wide range of nontumorous and neoplastic pancreatic tissues. In addition, possible regulators of SPARCL1, as well its effects on tumor growth and invasion, were investigated.

Materials and Methods

Tissue Samples

Pancreatic tissue specimens were obtained from patients with a median age of 71 years (range, 43–82 years) in whom resections for chronic pancreatitis (CP) or pancreatic tumors were performed. Normal pancreatic (NP) tissue samples were obtained from previously healthy individuals through an organ donor program. All samples were confirmed histologically. Freshly removed tissues (within 5 minutes of surgical excision) were fixed in paraformaldehyde solution for 12 to 24 hours and were subsequently embedded in paraffin for histologic analysis. Alternatively, tissue samples were embedded in Tissue-Tek OCT compound (Sakura Finetek, Torrance, CA) by freezing blocks in an acetone bath within liquid nitrogen and were stored at −80°C until use. Tissue arrays were constructed using a manual tissue arrayer (Beecher Instruments, Sun Prairie, WI). They contained 34 samples of primary PDAC and 8 samples of metastatic PDAC, as well as 9 samples of CP, 10 samples of noninflammed and nontumorous pancreatic tissues (each sample in triplicate sections to assure a reliable immunohistochemical expression profile [27]), and PanIN lesions of different grades (32 low-grade PanIN lesions and 12 high-grade PanIN lesions). In addition, a portion of the tissue samples was kept in RNAlater (Ambion Ltd., Huntingdon, Cambridgeshire, UK) or snap-frozen in liquid nitrogen immediately on surgical removal and was maintained at −80°C until use. The Human Subjects Committee of the University of Heidelberg (Heidelberg, Germany) and the University of Bern (Bern, Switzerland) approved all studies, and written informed consent was obtained from all patients.

Cell Culture

Pancreatic cancer cell lines were grown routinely in RPMI medium (Aspc-1, BxPc-3, Capan-1, Colo-357, SU8686, and T3M4) or DMEM (MiaPaCa-2 and Panc-1 cells), supplemented with 10% fetal bovine serum (FBS) and 100 U/ml penicillin (complete medium), and incubated in a 5% CO_2 humidified atmosphere. For induction experiments, 500 pM transforming growth factor (TGF) β1, 100 ng/ml bone morphogenetic protein (BMP) 2, 10 ng/ml fibroblast growth factor (FGF) 2, 500 ng/ml sonic hedgehog (Shh), 500 ng/ml Indian hedgehog (Ihh; R&D Systems GmbH, Wiesbaden-Nordenstadt, Germany), or 100 ng/ml tumor necrosis factor (TNF) α (Promega GmbH, Mannheim, Germany) was used.

Real-Time Quantitative Reverse Transcription–Polymerase Chain Reaction (qRT-PCR)

RT-PCR was performed using the LightCycler FastStart DNA SYBR Green kit, as previously described [28]. The number of specific transcripts was normalized to housekeeping genes (*cyclophilin B* and *HPRT*) and presented as adjusted transcripts per microliter of cDNA.

5-Aza-2′-Deoxycytidine (5aza-dC) Treatment

Pancreatic cancer cells were plated at a density of 1.5×10^6 cells per 10-cm tissue culture plate in complete medium and allowed to attach over a 24-hour period. 5aza-dC (Sigma-Aldrich Chemie GmbH, Schnelldorf, Germany) was added to a final concentration of 1 μM, and cells were cultured for 6 days. The medium was changed every other day. At the end of treatment, mRNA was extracted as described [29].

Cell Proliferation Assays

To assess pancreatic cancer cell proliferation, 3-(4,5-dimethylthiazol-2-yl)-2,5-diphenyltetrazolium bromide (MTT) assay was used as described previously [29].

Flow Cytometric Analysis

T3M4 and Panc-1 pancreatic cancer cells were plated in six-well plates (100,000 cells/well) and were incubated for indicated times with 8 or 125 ng/ml rSPARCL1. Cells were next harvested, washed with phosphate-buffered saline (PBS), and subsequently resuspended in 0.5 ml of hypotonic propidium iodide (PI) buffer (50 mg/ml PI, 0.1% Triton X-100, and 0.1% Na-citrate) or 2% PBS and stored overnight at 4°C. Measurements of DNA content or the dose toxicity of rSPARCL1 in each sample were performed with BD-LSR flow cytometer (Becton Dickinson and Co., Erembodegem-Aalst, Belgium).

In Vitro *Invasion Assays*

Briefly, BioCoat Matrigel (BD Biosciences, San Jose, CA) invasion chambers were rehydrated according to the manufacturer's instructions. Five hundred microliters of RPMI cell culture medium supplemented with 5% FBS and rSPARCL1 protein at the indicated concentration was added to the bottom of 24-well plates. Cells were seeded at a density of 5×10^4 cells/well into upper inserts. After 24 hours at 37°C, noninvading cells were removed from the upper surface of the separating membrane by gentle scrubbing with a cotton swab. Invading cells were fixed in 100% methanol and stained with 0.05% crystal violet in 20% ethanol. Membranes were mounted on glass slides and counted manually under a light microscope. The invasion index was calculated as the percentage of invaded cells in the treatment group compared to the percentage of invaded cells in the control group. All assays were performed in triplicate.

Laser Capture Microdissection (LCM) and Microarray Analysis

For this analysis, ductal cells were microdissected from NP ($n = 3$), CP ($n = 5$), and PDAC samples ($n = 6$). Tissue sections (6–8 μm thick) were prepared with a Reichard-Jung 1800 cryostat (Leica Microsystems GmbH, Wetzlar, Germany). LCM and RNA extraction were carried out as described previously [30]. In addition, RNA was extracted from 13 normal (nonmicrodissected) pancreatic tissues, 10 CP samples, 10 PDAC samples, and 10 samples of liver

metastasis of pancreatic cancer. The HG-U95Av2 array from Affymetrix (Santa Clara, CA) was used for this analysis. Poly(A)$^+$ RNA isolation, cDNA synthesis, cRNA *in vitro* transcription, and purification and fragmentation of obtained products were carried out as reported previously [30]. The hybridization of fragmented *in vitro* transcription products into oligonucleotide arrays was performed as recommended by the manufacturer.

Immunohistochemistry

Paraffin-embedded tissue sections 2–3 μm thick were deparaffinized in xylene and rehydrated in progressively decreasing concentrations of ethanol. Thereafter, the slides were placed in washing buffer (10 mM Tris–HCl, 0.85% NaCl, and 0.1% bovine serum albumin, pH 7.4) and subjected to immunostaining. Antigen retrieval was performed by boiling consecutive tissue sections in 10 mM citrate buffer for 10 minutes in a microwave oven. The sections were incubated with a goat polyclonal anti-SPARCL1 IgG (R&D Systems GmbH) or monoclonal mouse anti-human CD34 class IgG_1 (DAKO Corporation, Carpinteria, CA), as well as with normal goat IgG and normal mouse IgG_1 (DAKO Corporation) as negative controls, respectively. The slides were rinsed with washing buffer and incubated with anti-goat HRPO-conjugated IgG (Santa Cruz Biotechnology, Inc., Santa Cruz, CA) or anti-mouse HRPO-conjugated IgG (Amersham International, Buckinghamshire, UK) for 1 hour at room temperature. Tissue sections were washed, after which DAB–chromogen substrate mixture (DAKO Corporation) was applied. The slides were analyzed with the Axioplan 2 imaging microscope (Carl Zeiss, Göttingen, Germany). Microvessel counting was performed as previously described [31].

Immunoblotting

Cells were treated with 8 and 125 ng/ml rSPARCL1 for 48 hours, washed twice with ice-cold PBS, and lysed with lysis buffer (50 mM Tris–HCl, 100 mM NaCl, 2 mM EDTA, and 1% sodium dodecyl sulfate) containing one tablet of complete mini EDTA-free protease inhibitor cocktail (in 10-ml buffer; Roche Applied Science, Mannheim, Germany). Cell lysates (20 μg/lane) were separated on sodium dodecyl sulfate–polyacrylamide gels and electroblotted onto nitrocellulose membranes. The membranes were incubated in blocking solution (5% nonfat dry milk in 20 mM Tris–HCl, 150 mM NaCl, and 0.1% Tween-20), followed by incubation with mouse monoclonal anti–cyclin D1, rabbit polyclonal anti–cyclin E, or goat polyclonal anti-p21 (Santa Cruz Biotechnology, Inc.) overnight at 4°C. The membranes were washed in blocking solution and incubated with HRP-conjugated secondary antibodies for 1 hour at room temperature. Antibody detection was performed by an enhanced chemiluminescence reaction (Amersham International).

Statistical Analysis

Results are expressed as mean ± standard error of the mean (SEM), unless indicated otherwise. For statistical analysis, Student's *t* test or Mann-Whitney test was used, and significance was defined as $P < .05$. Spearman's *r* test was used for correlation analysis, and graphs were generated using GraphPad prism software (GraphPad Software, San Diego, CA).

Results

SPARCL1 Expression in Pancreatic Tissues

SPARCL1 mRNA expression levels were analyzed in NP tissues and compared to those of CP, PDAC, and diverse pancreatic tumors, using qRT-PCR. As shown in Figure 1, CP, PDAC, serous cystadenoma (SCA), mucinous cystadenoma (MCA), acinar cell carcinoma (ACC), and malignant neuroendocrine tumor (NET) exhibited higher median SPARCL1 mRNA levels compared to NP. In contrast, intraductal papillary mucinous neoplasm (IPMN) and benign NETs exhibited median SPARCL1 mRNA levels lower than those of NP. The highest median RNA levels (11,248 copies/μl cDNA) were observed in pancreatic SCA, and the lowest median RNA levels (651 copies/μl cDNA) were observed in benign neuroendocrine pancreatic tumor tissues. Interestingly, there was a tendency of higher median SPARCL1

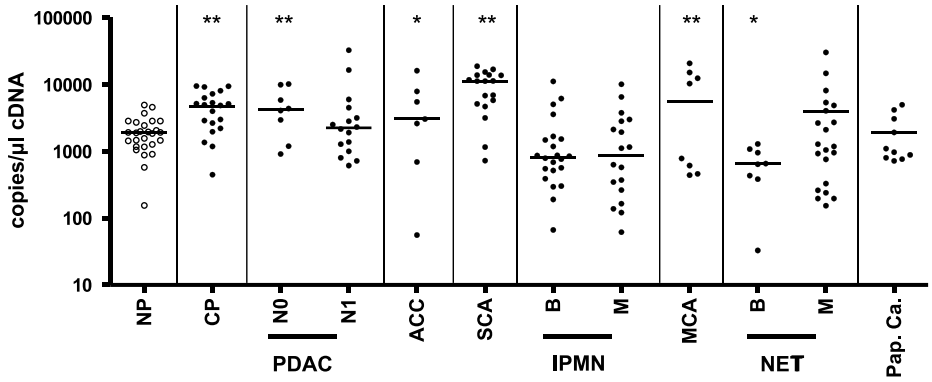

Figure 1. *SPARCL1 mRNA expression in the pancreas. RNA was extracted from normal (NP), CP, and PDAC without (N_0) or with (N_1) lymph node metastasis, ACC, SCA, benign (B) and malignant (M) IPMN, MCA, benign (B) and malignant (M) NETs, and ampullary carcinoma, as described in the Materials and Methods section. RNA input was normalized to the average expression of the two housekeeping genes* HPRT *and* cyclophilin B*, and is presented as copy number per microliter of cDNA. Horizontal lines represent the median value. *P < .05, **P < .01, compared to NP.*

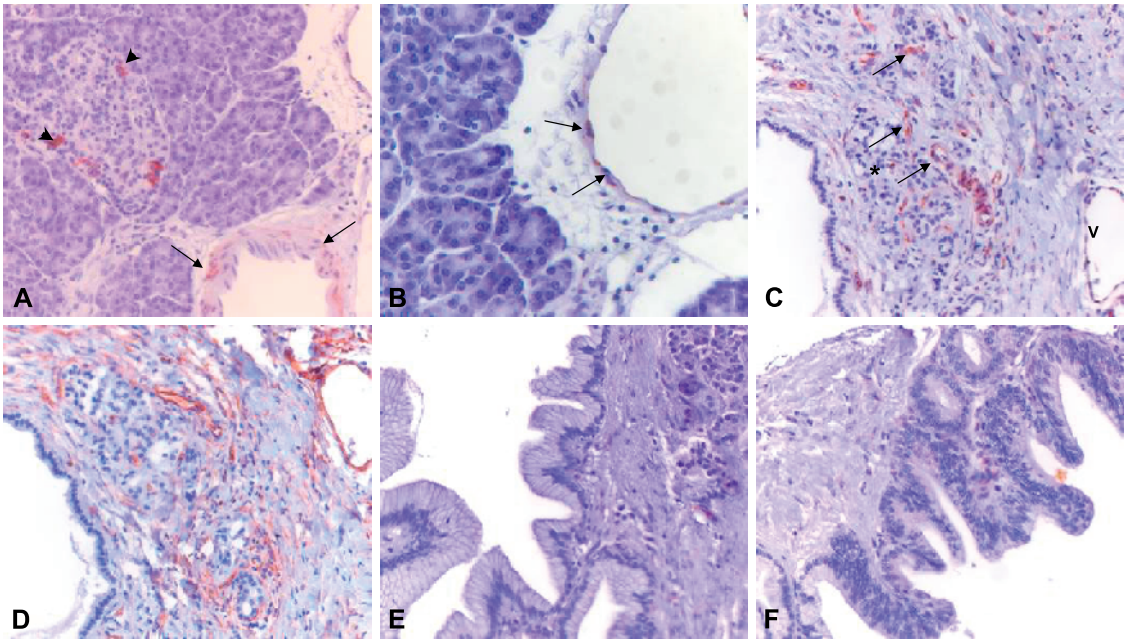

Figure 2. *Immunohistochemical detection of SPARCL1 and CD34 in benign pancreatic tissues. Immunostaining of paraffin-embedded tissue sections was performed using the indirect peroxidase technique, as described in the Materials and Methods section. In the normal pancreas, SPARCL1 was detected in some of the islet cells (A; arrowhead), in the muscular layer (A; arrows), and in the endothelium of preexisting vessels (B; arrows). In addition, in CP, specific staining of microvessels in areas of tissue remodeling was seen (C; arrows) (microvessels: asterisk, area of tissue remodeling; V, preexisting vein). No staining was detected in low-grade PanIN lesions (E and F). CD34 staining (D) was used to confirm the specificity of SPARCL1 vascular staining (Figure 4).*

mRNA levels in N_0 PDAC compared to N_1 PDAC cases, and in malignant compared to benign NETs, but this tendency did not reach statistical significance. In contrast, there was no difference in SPARCL1 mRNA levels between benign and malignant IPMN cases (Figure 1).

Next, SPARCL1 was localized by immunohistochemistry to identify the source of SPARCL1 in different pancreatic tissues. Immunohistochemistry revealed that SPARCL1 was localized in some of the islet cells and in endothelial and smooth muscle cells of small-sized and medium-sized blood vessels (Figure 2, *A* and *B*), including small capillaries in areas of inflammation/tumor growth. Interestingly, benign and inflammatory pancreatic tissues, such as CP (Figure 2*C*), SCA (Figure 3*C*), IPMN, and MCA, exhibited stronger SPARCL1 staining in vascular structures compared to PDAC. In contrast, SPARCL1 was below the level of detection in other structures of pancreatic tissues, especially in cancer cells in PDAC, tubular complexes, and stromal fibrous tissue elements in both CP (Figure 2*C*) and PDAC tissues (Figure 3*B*). Interestingly, all PanIN-3 lesions ($n = 5$) exhibited a specific localization pattern in small capillaries under the basement membrane, whereas all PanIN-1A ($n = 16$), 14 of 16 PanIN-1B, and 5 of 7 PanIN-2 lesions did not show this expression pattern (Figure 2*E* and *F*; Figure 3*A*). Comparable results were obtained with two additional antibodies: polyclonal goat anti-rat SC-1 (Santa Cruz Biotechnology, Inc.) and rat monoclonal anti-mouse SC-1 [32].

To confirm the specificity of SPARCL1 vascular staining and to quantify SPARCL1 expression in different pancreatic tissues, we stained consecutive pancreatic tissue sections with the endothelial marker CD34 [33]. Tissues were obtained from samples of CP, PDAC, and three types of benign cystic tumors (IPMN, SCA, and MCA). This analysis revealed that SPARCL1 staining was specific for vascular structures in pancreatic tissues (Figure 2*D*; Figure 3, *D* and *F*). Systematic counting of vessels revealed that: 1) the extent of vascularization according to the expression of CD34 was similar in different samples, and 2) SPARCL1 was expressed in 15.4 ± 1.6% (PDAC), 32.4 ± 1.4% (CP), 40.4 ± 6.3% (benign IPMN), 66 ± 1.4% (SCA), and 29.9 ± 1.2% (MCA) of CD34-positive microvessels (Figure 4). Higher levels of the vascular expression of SPARCL1 were therefore identified in chronic inflammatory condition (CP) and benign pancreatic cystic tumors (IPMN, SCA, and MCA) compared to invasive pancreatic cancer (PDAC), despite a similar overall density of CD34-positive vessels.

To confirm absent/low SPARCL1 levels in pancreatic cancer cells, we asked whether SPARCL1 mRNA was expressed in cancer cells themselves by the use of LCM and microarray analysis of microdissected ductal cells. The mean SPARCL1 mRNA levels in NP (bulk) tissues ($n = 13$) were set to 100. In comparison to the expression in normal tissues, the mean SPARCL1 mRNA levels were 152 in NP ducts ($n = 3$), 120 in CP ductal cells ($n = 5$), and 67 in microdissected cancer cells ($n = 6$) (Figure 5*A*). Thus, SPARCL1 expression is reduced in pancreatic cancer cells compared to NP ductal cells. In addition, microarray analysis of CP and PDAC bulk tissues, as well as of pancreatic cancer metastasis to the liver, demonstrated an increase in mean SPARCL1 mRNA levels in CP (144) and PDAC (186)

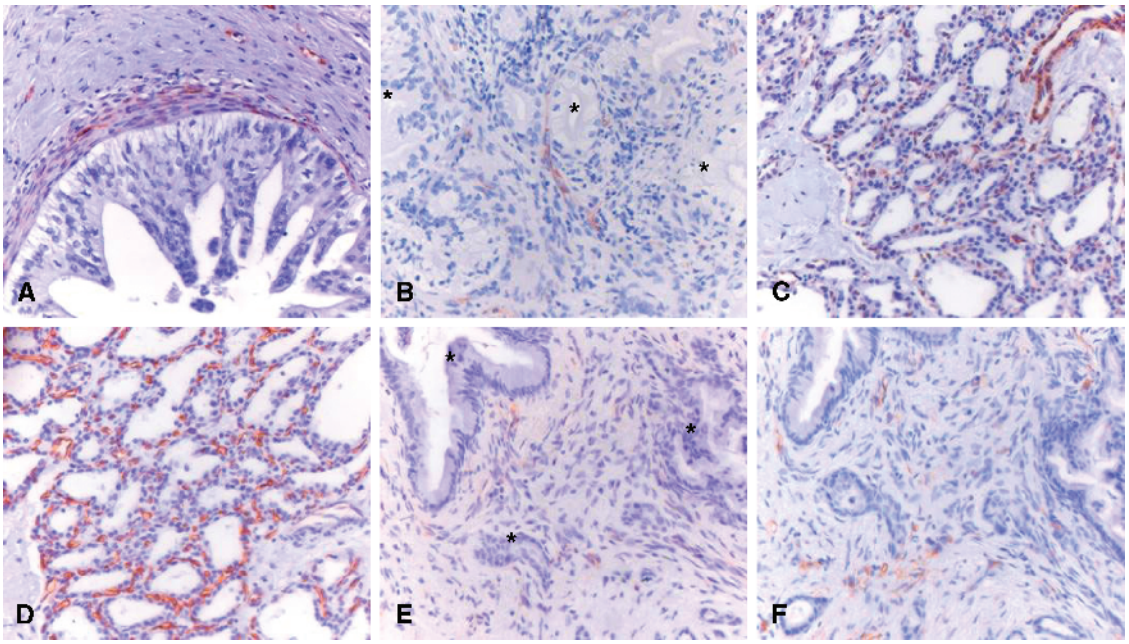

Figure 3. *Immunohistochemical detection of SPARCL1 and CD34 in neoplastic pancreatic tissues. Immunostaining of paraffin-embedded tissue sections was performed using the indirect peroxidase technique, as described in the Materials and Methods section. High-grade PanIN showed SPARCL1-positive microvessels under the basement membrane (A). Ductal adenocarcinoma cells were always negative (B and E; asterisk); weak to moderate staining was detected in some of the small vessels of the tumor stroma (B and E). Benign pancreatic tumors, such as SCA, displayed moderate staining in numerous microvessels of the tumor stroma (C). CD34 staining (D and F) was used to confirm the specificity of SPARCL1 vascular staining (Figure 4).*

compared to NP tissues (set to 100), which is in agreement with qRT-PCR data and further confirms that SPARCL1 is differentially expressed in PDAC. Interestingly, however, the mean SPARCL1 mRNA level was reduced (54) in liver metastases of pancreatic cancer (Figure 5*B*). To further analyze this aspect, immunohistochemistry was carried out in samples of pancreatic cancer metastasis to the liver ($n = 10$), lymph nodes ($n = 4$), and peritoneum ($n = 9$). This analysis revealed absent SPARCL1 staining in metastatic cancer cells and occasional SPARCL1 expression in associated tumor capillaries (Figure 6).

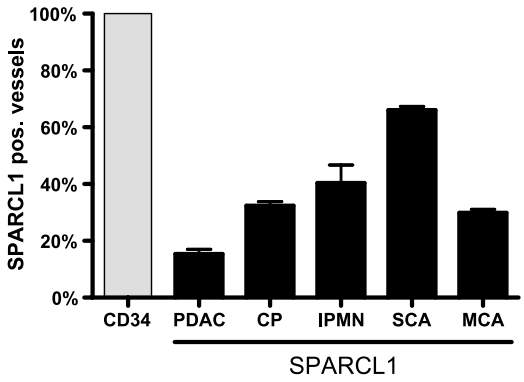

Figure 4. *Semiquantification of SPARCL1/CD34 vascular expression in pancreatic tissues by immunohistochemistry. SPARCL1 and CD34 immunohistochemistry was performed in consecutive pancreatic tissue sections from PDAC, CP, IPMN, SCA, and MCA, as described in the Materials and Methods section. SPARCL1 vascular expression was evaluated in these tissues (gray columns) compared to CD34 expression (black column). Values represent the mean ± SEM of the number of vessels counted in three different areas (×20 per high-power field).*

SPARCL1 Expression and Transcriptional Regulation in Pancreatic Cancer Cells

qRT-PCR analysis of eight cultured pancreatic cancer cell lines showed essentially no SPARCL1 mRNA in four of eight pancreatic cancer cells and low mRNA levels in four of eight pancreatic cancer cells, with a range of 2.8 to 40.5 copies/μl cDNA (Figure 7*A*). Immunocytochemistry was performed on eight pancreatic cancer cells, in which SPARCL1 was below the level of detection in all tested cells (data not shown). To exclude SPARCL1 promoter hypermethylation as a cause of low transcript levels, we treated all pancreatic cancer cells with a 5aza-dC demethylation reagent, followed by qRT-PCR analysis. This analysis revealed a 3.2-fold, 3.8-fold, and 1.1-fold increase in SPARCL1 mRNA expression in Colo-357, SU8686, and T3M4 cells, respectively (Figure 7*A*), and no effect in the other five cell lines. Thus, promoter hypermethylation is not the dominant mechanism of the observed low to absent SPARCL1 expression in pancreatic cancer cells.

The regulation of SPARCL1 mRNA expression by a number of growth factors and cytokines that are known to influence the behavior of pancreatic cancer cells [34,35] was examined. Analysis revealed that SPARCL1 mRNA expression was not affected in any of the pancreatic cancer cells tested, with the exception of T3M4 cells. In this cell line, SPARCL1 mRNA was induced by Ihh (500 ng/ml), Shh (500 ng/ml), and FGF-2 (10 ng/ml), with effects (percentage of control) of +91.7 ± 2.7%, +59.3 ± 8.1%, and +46 ± 4.9%, respectively. Treatment of T3M4 cells with TNF-α (100 ng/ml) reduced SPARCL1

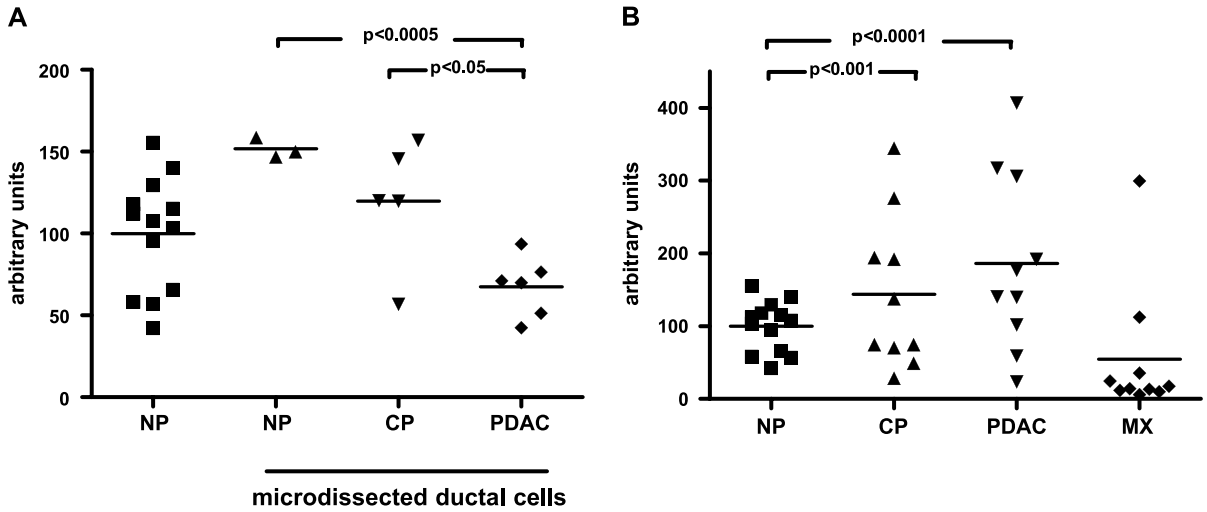

Figure 5. *(A) SPARCL1 mRNA expression in microdissected pancreatic ductal cells. Microarray analysis for the mRNA levels of SPARCL1 from NP tissues (n = 13), NP ducts (n = 3), ducts from CP tissues (n = 5), and cancer cells (n = 6). Values represent arbitrary units normalized to housekeeping genes [30] and NP tissues (mean set to 100). (B) SPARCL1 mRNA expression in bulk pancreatic tissues. Microarray analysis for the mRNA levels of SPARCL1 from NP tissues (n = 13), CP (n = 10), PDAC tissues (n = 10), and liver metastases of pancreatic cancer (n = 10). Values represent arbitrary units normalized to housekeeping genes [30] and NP tissues (mean set to 100). Horizontal bars represent mean values.*

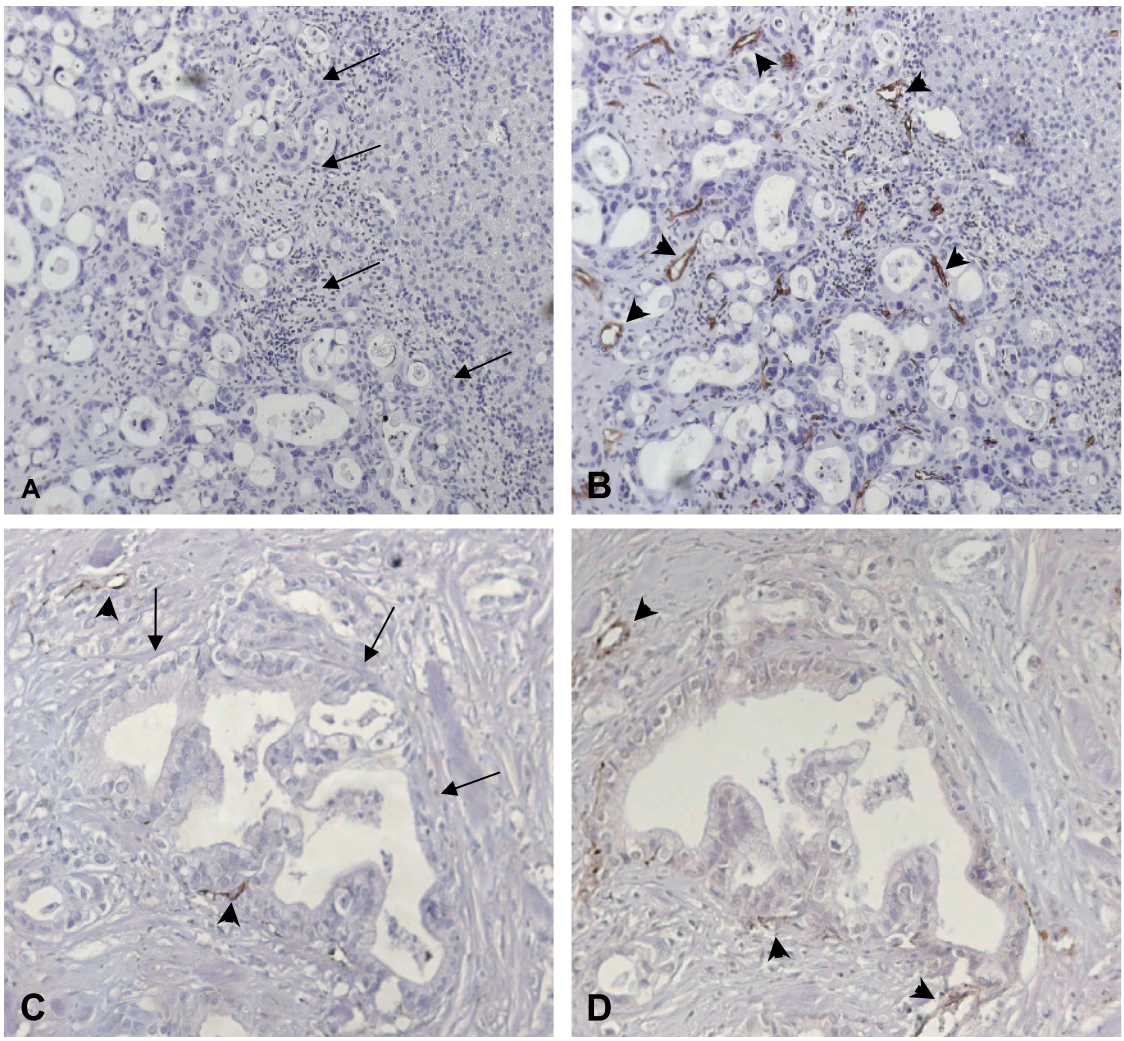

Figure 6. *Immunohistochemical detection of SPARCL1 and CD34 in metastatic pancreatic cancer. Immunostaining of paraffin-embedded tissue sections was performed using the indirect peroxidase technique, as described in the Materials and Methods section. Liver metastasis (A and B) and lymph node metastasis (C and D). Note the absence of SPARCL1 staining in metastatic cancer cells (A and C; arrows). Occasionally, blood vessels were SPARCL1-positive (C; arrowheads). CD34 staining was used to identify blood vessels (B and D; arrowheads).*

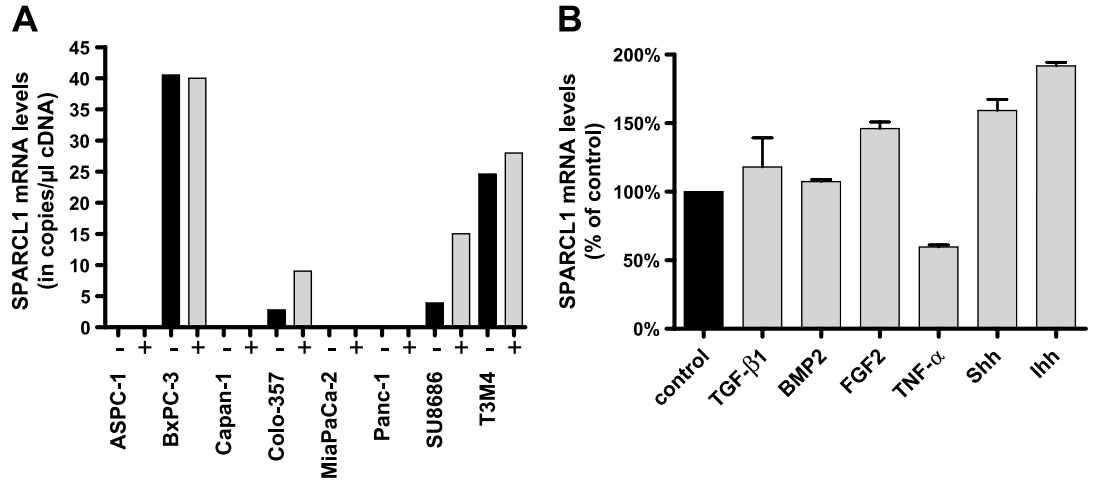

Figure 7. *SPARCL1 mRNA expression in pancreatic cancer cell lines. (A) Real-time qRT-PCR analysis of SPARCL1 mRNA levels in pancreatic cancer cell lines. mRNA was extracted from eight pancreatic cancer cell lines without (black column) or with (gray column) treatment with 5aza-dC demethylation reagent, as described in the Materials and Methods section. (B) Transcriptional regulation of SPARCL1 by cytokines and growth factors. T3M4 pancreatic cancer cells were treated with TGF-β1, BMP-2, FGF-2, TNF-α, Shh, and Ihh (gray columns), or were not treated (black column). RNA was extracted, and qRT-PCR was performed as described in the Materials and Methods section. Values represent the mean ± SEM of three independent experiments. RNA input was normalized to the average expression of the two housekeeping genes* HPRT *and* cyclophilin B*, and is presented as copy number per microliter of cDNA.*

mRNA significantly by 40.3 ± 1.6%. TGF-β1 (500 pM) and BMP-2 (100 ng/ml) did not significantly influence SPARCL1 mRNA levels in T3M4 cells (Figure 7*B*).

SPARCL1 Reduces the Invasion of Pancreatic Cancer Cells

We next asked whether the treatment of two pancreatic cancer cell lines (T3M4 and Panc-1) with rSPARCL1 affected proliferation or invasiveness. MTT assays revealed a concentration-dependent inhibition of growth with maximum effects of 35.5 ± 3.9% in T3M4 and 38.2 ± 6.5% in Panc-1 cells at 125 ng/ml (1.28 nM) rSPARCL1 (Figure 8, *A* and *B*). PI staining of T3M4 and Panc-1 cells excluded potential toxic effects of rSPARCL1 (data not shown). Fluorescence-activated cell sorter analysis was performed to investigate a mechanism by which the proliferation of T3M4 and Panc-1 cells was reduced. Although T3M4 cells did not show detectable changes in cell cycle in response to rSPARCL1 after 48 hours, Panc-1 cells exhibited a minor (+2% and +5.2%) accumulation in G_0/G_1 phase at a concentration of 8 and 125 ng/ml rSPARCL1 after 48 hours, respectively (data not shown). These effects were not accompanied by changes in the expression of cell cycle–regulatory proteins cyclins D1 and E, or the tumor-suppressor protein p21 (data not shown). There was no apoptotic cell death induced by rSPARCL1 in both Panc-1 and T3M4 cells at indicated concentrations and duration of treatment.

Matrigel invasion assays were performed on T3M4 and Panc-1 cells in the presence or in the absence of indicated concentrations of rSPARCL1 (Figure 9). rSPARCL1 reduced invasion by 68.5 ± 2.8% in T3M4 cells, and by 34.2 ± 1.8% in Panc-1 cells, at a concentration of 8 ng/ml. The inhibitory effects were less pronounced at 125 ng /ml rSPARCL1, at which T3M4 exhibited reduction in invasion by 44.4 ± 7.4% and Panc-1 exhibited reduction in invasion by 26.8 ± 1.2% (Figure 9).

Discussion

The expression of SPARCL1, which is an abundant matricellular protein that modulates high endothelial cell adhesion to

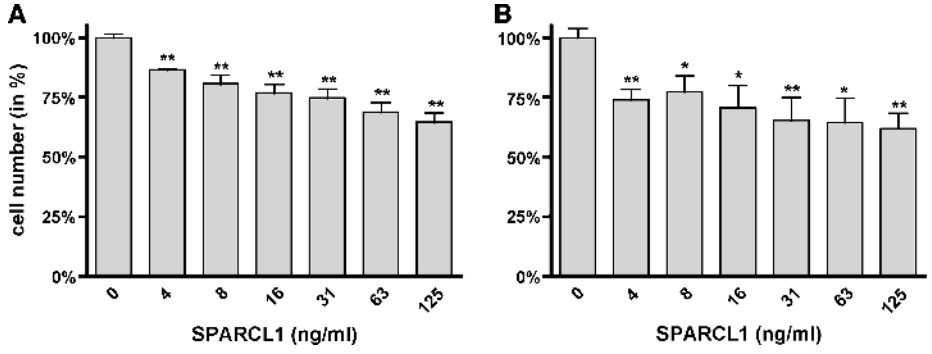

Figure 8. *The effects of rSPARCL1 on the proliferation of (A) T3M4 and (B) Panc-1 pancreatic cancer cells, as determined by the MTT assay. Pancreatic cancer cells were incubated with rSPARCL1 at the indicated concentrations (in ng/ml) for 48 hours before analysis. Data are expressed as the percentage of change compared to controls, and are plotted as the mean ± SEM of three independent experiments. *P < .05, **P < .01, compared to controls.*

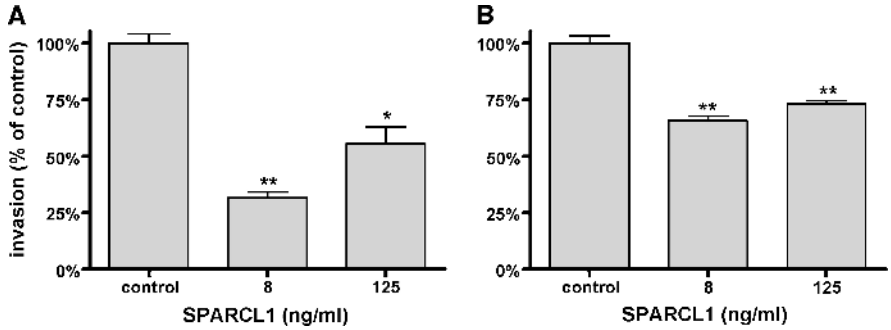

Figure 9. *The effects of rSPARCL1 on the invasion of T3M4 and Panc-1 pancreatic cancer cells. (A) T3M4 and (B) Panc-1 pancreatic cancer cells were incubated with 0, 8, or 125 ng/ml rSPARCL1 for 24 hours. Invasion was analyzed by Matrigel invasion assays, as described in the Materials and Methods section. Data are presented as the percentage of invasion compared to control cells (100%) and are plotted as the mean ± SEM of three independent experiments. *P < .05, **P < .01, compared to controls.*

the basement membrane and may facilitate lymphocytic migration/extravasation [2,36], is deregulated in various tumors. The results of the present study show that SPARCL1 mRNA expression in NP tissues was mainly accounted for in islets together with preexistent vascular structures. The median SPARCL1 mRNA levels were increased in PDAC tissues compared to NP tissues, a change due specifically to the expression of SPARCL1 in small vessels formed as a result of neoangiogenesis in PDAC tissues. This finding is in accordance with previous observations showing SPARCL1 as a marker of angioendothelial cells in pancreatic cancer [37]. Furthermore, benign and inflammatory pancreatic lesions such as CP, SCA, and MCA tissues (the last two characterized by CP-like changes in the surrounding stroma, with tissue remodeling and neoangiogenesis) [38,39] expressed higher levels of SPARCL1 mRNA than were observed in PDAC tissues and liver metastases of PDAC. These data indicate that SPARCL1 expression in inflammatory and neoplastic pancreatic lesions depends on the extent of neovascularization, regardless of the type of lesion. The lower levels of SPARCL1 mRNA in PDAC tissues (primary and also metastatic) compared to CP and benign cystic lesions could be due to its downregulation, as has been described in other human cancers. SPARCL1 contributes to the induction or maintenance of the features of the high endothelial venule endothelium that facilitates lymphocyte migration [2] and provides immune surveillance [40]. Thus, increased expression of SPARCL1 in reactive vascular structures in benign and inflammatory lesions might contribute to the support of immune response in these lesions [41]. In contrast, decreased or lost expression of SPARCL1 in reactive vessels in PDAC might alter the permeability of the endothelium and the extravasation of immune cells, thus impairing immune response against cancer cells in PDAC tissues [2,36]. Additionally, the higher SPARCL1 mRNA levels in microdissected ductal cells from NP and CP tissues compared to pancreatic cancer cells, as well as the low-to-absent SPARCL1 mRNA levels in cultured pancreatic cancer cell lines and the liver metastases of pancreatic cancer, provide further support to the hypothesis that SPARCL1 acts as a tumor suppressor, the expression of which is lost in PDAC cells.

The mechanisms of SPARCL1 downregulation in PDAC are not completely understood. Promoter hypermethylation is one of the factors that mask the expression of genes in pancreatic cancer [42]. SPARCL1 promoter demethylation increased SPARCL1 mRNA levels in three of eight pancreatic cancer cell lines, but these increased levels were still approximately 100-fold lower than those observed in bulk pancreatic cancer tissues, an observation suggesting that promoter hypermethylation is not the key mechanism by which SPARCL1 expression is repressed in pancreatic cancer cells.

Transcriptional regulation of SPARCL1 by other factors such as cytokines may be another reason for the reduced expression of SPARCL1 mRNA in pancreatic cancer cells. Supporting this theory, SPARCL1 transcription was regulated by proteins that show frequent derangement in PDAC, such as FGF-2 [43], TNF-α [44], Shh [45], and Ihh [46,29]. Surprisingly, SPARCL1 mRNA expression levels were decreased in response to TNF-α (a factor with antiproliferative effects on pancreatic cancer cells) [47] and were increased in response to other factors that have mitogenic effects on pancreatic cancer cells, such as FGF-2 [43], Shh [45], and Ihh [29]. Nevertheless, these effects were observed in only one of eight cell lines and were quite minimal. The maximum increase in SPARCL1 mRNA was less than two-fold, and basal levels of SPARCL1 mRNA in T3M4 cells were only 24.6 copies/μl cDNA. Thus, the effects of SPARCL1 on pancreatic cancer cells are paracrine rather than autocrine (i.e., SPARCL1 produced by endothelia, but not by cancer cells, affects pancreatic cancer cell invasion). Antiadhesive effects on pancreatic cancer cells were confirmed using rSPARCL1. Ideally, this observation could further be substantiated by knock-down and knock-in experiments. However, SPARCL1 expression levels were too low in cultured pancreatic cancer cells for further knock-down experiments. However, forced overexpression of SPARCL1 on the protein level has not been achieved in cultured cell lines (Weaver et al., unpublished observation). Nonetheless, we believe that the antiadhesive effects observed with rSPARCL1 in pancreatic cancer cells represent a true physiologic effect.

Analysis of SPARCL1 in PanIN lesions allowed two important observations. First, a significant level of neoangiogenesis was associated mainly with high-grade lesions,

indicating a prominent stromal remodeling in the immediate preinvasive stage. Second, the downregulation of SPARCL1 takes place in the late stage of pancreatic cancer progression. That downregulation is a late event was also supported by the finding that N_1 PDAC cases showed a tendency for lower SPARCL1 mRNA levels compared to N_0 PDAC cases, as has been shown for metastatic prostate carcinoma [22].

In conclusion, SPARCL1 expression in pancreatic tissues corresponds to vascular content. SPARCL1 is downregulated in PDAC cells, and supplementation of these cells with rSPARCL1 has anti-invasive effects, supporting a tumor-suppressor function for this matricellular protein.

References

[1] Findlay DM, Fisher LW, McQuillan CI, Termine JD, and Young MF (1988). Isolation of the osteonectin gene: evidence that a variable region of the osteonectin molecule is encoded within one exon. *Biochemistry* **27,** 1483–1489.

[2] Girard JP and Springer TA (1995). Cloning from purified high endothelial venule cells of hevin, a close relative of the antiadhesive extracellular matrix protein SPARC. *Immunity* **2,** 113–123.

[3] Johnston IG, Paladino T, Gurd JW, and Brown IR (1990). Molecular cloning of SC1: a putative brain extracellular matrix glycoprotein showing partial similarity to osteonectin/BM40/SPARC. *Neuron* **4,** 165–176.

[4] Sullivan MM and Sage EH (2004). Hevin/SC1, a matricellular glycoprotein and potential tumor-suppressor of the SPARC/BM-40/Osteonectin family. *Int J Biochem Cell Biol* **36,** 991–996.

[5] Swaroop A, Hogan BL, and Francke U (1988). Molecular analysis of the cDNA for human SPARC/osteonectin/BM-40: sequence, expression, and localization of the gene to chromosome 5q31–q33. *Genomics* **2,** 37–47.

[6] Bornstein P and Sage EH (2002). Matricellular proteins: extracellular modulators of cell function. *Curr Opin Cell Biol* **14,** 608–616.

[7] Bradshaw AD, Graves DC, Motamed K, and Sage EH (2003). SPARC-null mice exhibit increased adiposity without significant differences in overall body weight. *Proc Natl Acad Sci USA* **100,** 6045–6050.

[8] Brekken RA, Puolakkainen P, Graves DC, Workman G, Lubkin SR, and Sage EH (2003). Enhanced growth of tumors in SPARC null mice is associated with changes in the ECM. *J Clin Invest* **111,** 487–495.

[9] Goldblum SE, Ding X, Funk SE, and Sage EH (1994). SPARC (secreted protein acidic and rich in cysteine) regulates endothelial cell shape and barrier function. *Proc Natl Acad Sci USA* **91,** 3448–3452.

[10] Sullivan MM, Barker TH, Funk SE, Karchin A, Seo NS, Hook M, Sanders J, Starcher B, Wight TN, Puolakkainen P, et al. (2006). Matricellular hevin regulates decorin production and collagen assembly. *J Biol Chem* **281,** 27621–27632.

[11] Gilmour DT, Lyon GJ, Carlton MB, Sanes JR, Cunningham JM, Anderson JR, Hogan BL, Evans MJ, and Colledge WH (1998). Mice deficient for the secreted glycoprotein SPARC/osteonectin/BM40 develop normally but show severe age-onset cataract formation and disruption of the lens. *EMBO J* **17,** 1860–1870.

[12] Porte H, Chastre E, Prevot S, Nordlinger B, Empereur S, Basset P, Chambon P, and Gespach C (1995). Neoplastic progression of human colorectal cancer is associated with overexpression of the *stromelysin-3* and *BM-40/SPARC* genes. *Int J Cancer* **64,** 70–75.

[13] Porte H, Triboulet JP, Kotelevets L, Carrat F, Prevot S, Nordlinger B, DiGioia Y, Wurtz A, Comoglio P, Gespach C, et al. (1998). Overexpression of *stromelysin-3*, *BM-40/SPARC*, and *MET* genes in human esophageal carcinoma: implications for prognosis. *Clin Cancer Res* **4,** 1375–1382.

[14] Le Bail B, Faouzi S, Boussarie L, Guirouilh J, Blanc JF, Carles J, Bioulac-Sage P, Balabaud C, and Rosenbaum J (1999). Osteonectin/SPARC is overexpressed in human hepatocellular carcinoma. *J Pathol* **189,** 46–52.

[15] Bellahcene A and Castronovo V (1995). Increased expression of osteonectin and osteopontin, two bone matrix proteins, in human breast cancer. *Am J Pathol* **146,** 95–100.

[16] Jacob K, Webber M, Benayahu D, and Kleinman HK (1999). Osteonectin promotes prostate cancer cell migration and invasion: a possible mechanism for metastasis to bone. *Cancer Res* **59,** 4453–4457.

[17] Yamanaka M, Kanda K, Li NC, Fukumori T, Oka N, Kanayama HO, and Kagawa S (2001). Analysis of the gene expression of SPARC and its prognostic value for bladder cancer. *J Urol* **166,** 2495–2499.

[18] Ledda F, Bravo AI, Adris S, Bover L, Mordoh J, and Podhajcer OL (1997). The expression of the secreted protein acidic and rich in cysteine (SPARC) is associated with the neoplastic progression of human melanoma. *J Invest Dermatol* **108,** 210–214.

[19] Rempel SA, Golembieski WA, Ge S, Lemke N, Elisevich K, Mikkelsen T, and Gutierrez JA (1998). SPARC: a signal of astrocytic neoplastic transformation and reactive response in human primary and xenograft gliomas. *J Neuropathol Exp Neurol* **57,** 1112–1121.

[20] Rempel SA, Ge S, and Gutierrez JA (1999). SPARC: a potential diagnostic marker of invasive meningiomas. *Clin Cancer Res* **5,** 237–241.

[21] Guweidhi A, Kleeff J, Adwan H, Giese NA, Wente MN, Giese T, Buchler MW, Berger MR, and Friess H (2005). Osteonectin influences growth and invasion of pancreatic cancer cells. *Ann Surg* **242,** 224–234.

[22] Nelson PS, Plymate SR, Wang K, True LD, Ware JL, Gan L, Liu AY, and Hood L (1998). Hevin, an antiadhesive extracellular matrix protein, is down-regulated in metastatic prostate adenocarcinoma. *Cancer Res* **58,** 232–236.

[23] Bendik I, Schraml P, and Ludwig CU (1998). Characterization of MAST9/Hevin, a SPARC-like protein, that is down-regulated in non–small cell lung cancer. *Cancer Res* **58,** 626–629.

[24] Claeskens A, Ongenae N, Neefs JM, Cheyns P, Kaijen P, Cools M, and Kutoh E (2000). Hevin is down-regulated in many cancers and is a negative regulator of cell growth and proliferation. *Br J Cancer* **82,** 1123–1130.

[25] St Croix B, Rago C, Velculescu V, Traverso G, Romans KE, Montgomery E, Lal A, Riggins GJ, Lengauer C, Vogelstein B, et al. (2000). Genes expressed in human tumor endothelium. *Science* **289,** 1197–1202.

[26] Isler SG, Schenk S, Bendik I, Schraml P, Novotna H, Moch H, Sauter G, and Ludwig CU (2001). Genomic organization and chromosomal mapping of *SPARC-like 1*, a gene down regulated in cancers. *Int J Oncol* **18,** 521–526.

[27] Shergill IS, Shergill NK, Arya M, and Patel HR (2004). Tissue microarrays: a current medical research tool. *Curr Med Res Opin* **20,** 707–712.

[28] Kayed H, Kleeff J, Keleg S, Buchler MW, and Friess H (2003). Distribution of Indian hedgehog and its receptors patched and smoothened in human chronic pancreatitis. *J Endocrinol* **178,** 467–478.

[29] Kayed H, Kleeff J, Keleg S, Guo J, Ketterer K, Berberat PO, Giese N, Esposito I, Giese T, Buchler MW, et al. (2004). Indian hedgehog signaling pathway: expression and regulation in pancreatic cancer. *Int J Cancer* **110,** 668–676.

[30] Ketterer K, Rao S, Friess H, Weiss J, Buchler MW, and Korc M (2003). Reverse transcription–PCR analysis of laser-captured cells points to potential paracrine and autocrine actions of neurotrophins in pancreatic cancer. *Clin Cancer Res* **9,** 5127–5136.

[31] Esposito I, Menicagli M, Funel N, Bergmann F, Boggi U, Mosca F, Bevilacqua G, and Campani D (2004). Inflammatory cells contribute to the generation of an angiogenic phenotype in pancreatic ductal adenocarcinoma. *J Clin Pathol* **57,** 630–636.

[32] Brekken RA, Sullivan MM, Workman G, Bradshaw AD, Carbon J, Siadak A, Murri C, Framson PE, and Sage EH (2004). Expression and characterization of murine hevin (SC1), a member of the SPARC family of matricellular proteins. *J Histochem Cytochem* **52,** 735–748.

[33] Simmons DL, Satterthwaite AB, Tenen DG, and Seed B (1992). Molecular cloning of a cDNA encoding CD34, a sialomucin of human hematopoietic stem cells. *J Immunol* **148,** 267–271.

[34] Kayed H, Kleeff J, Osman T, Keleg S, Buchler MW, and Friess H (2006). Hedgehog signaling in the normal and diseased pancreas. *Pancreas* **32,** 119–129.

[35] Korc M (1998). Role of growth factors in pancreatic cancer. *Surg Oncol Clin North Am* **7,** 25–41.

[36] Girard JP and Springer TA (1996). Modulation of endothelial cell adhesion by hevin, an acidic protein associated with high endothelial venules. *J Biol Chem* **271,** 4511–4517.

[37] Iacobuzio-Donahue CA, Ryu B, Hruban RH, and Kern SE (2002). Exploring the host desmoplastic response to pancreatic carcinoma: gene expression of stromal and neoplastic cells at the site of primary invasion. *Am J Pathol* **160,** 91–99.

[38] Kosmahl M, Wagner J, Peters K, Sipos B, and Kloppel G (2004). Serous cystic neoplasms of the pancreas: an immunohistochemical analysis revealing alpha-inhibin, neuron-specific enolase, MUC6 as new markers. *Am J Surg Pathol* **28,** 339–346.

[39] Zamboni G, Scarpa A, Bogina G, Iacono C, Bassi C, Talamini G, Sessa F, Capella C, Solcia E, Rickaert F, et al. (1999). Mucinous cystic tumors

of the pancreas: clinicopathological features, prognosis, and relationship to other mucinous cystic tumors. *Am J Surg Pathol* **23,** 410–422.

[40] Picker LJ (1992). Mechanisms of lymphocyte homing. *Curr Opin Immunol* **4,** 277–286.

[41] Barker TH, Framson P, Puolakkainen PA, Reed M, Funk SE, and Sage EH (2005). Matricellular homologs in the foreign body response: hevin suppresses inflammation, but hevin and SPARC together diminish angiogenesis. *Am J Pathol* **166,** 923–933.

[42] Okami J, Simeone DM, and Logsdon CD (2004). Silencing of the hypoxia-inducible cell death protein BNIP3 in pancreatic cancer. *Cancer Res* **64,** 5338–5346.

[43] Yamanaka Y, Friess H, Buchler M, Beger HG, Uchida E, Onda M, Kobrin MS, and Korc M (1993). Overexpression of acidic and basic fibroblast growth factors in human pancreatic cancer correlates with advanced tumor stage. *Cancer Res* **53,** 5289–5296.

[44] Watanabe N, Tsuji N, Tsuji Y, Sasaki H, Okamoto T, Akiyama S, Kobayashi D, Sato T, Yamauchi N, and Niitsu Y (1996). Endogenous tumor necrosis factor inhibits the cytotoxicity of exogenous tumor necrosis factor and adriamycin in pancreatic carcinoma cells. *Pancreas* **13,** 395–400.

[45] Thayer SP, di Magliano MP, Heiser PW, Nielsen CM, Roberts DJ, Lauwers GY, Qi YP, Gysin S, Fernandez-del Castillo C, Yajnik V, et al. (2003). Hedgehog is an early and late mediator of pancreatic cancer tumorigenesis. *Nature* **425,** 851–856.

[46] Berman DM, Karhadkar SS, Maitra A, Montes De Oca R, Gerstenblith MR, Briggs K, Parker AR, Shimada Y, Eshleman JR, Watkins DN, et al. (2003). Widespread requirement for Hedgehog ligand stimulation in growth of digestive tract tumours. *Nature* **425,** 846–851.

[47] Schmiegel WH, Caesar J, Kalthoff H, Greten H, Schreiber HW, and Thiele HG (1988). Antiproliferative effects exerted by recombinant human tumor necrosis factor-alpha (TNF-alpha) and interferon-gamma (IFN-gamma) on human pancreatic tumor cell lines. *Pancreas* **3,** 180–188.